



**NEUTRONICS STUDY ON THE JAERI 5 MW SPALLATION  
NEUTRON SOURCE**  
**– NEUTRONIC PERFORMANCE OF THE REFERENCE  
TARGET-MODERATOR-REFLECTOR SYSTEM  
AND THE TARGET SHAPE/SIZE EFFECTS –**

**March 1999**

**Makoto TESHIGAWARA, Noboru WATANABE,  
Hiroshi TAKADA, Tetsuya KAI, Hiroshi NAKASHIMA,  
Tadashi NAGAO, Yukio OYAMA, Yujiro IKEDA and  
Kazuaki KOSAKO\***

本レポートは、日本原子力研究所が不定期に公開している研究報告書です。  
入手の問合わせは、日本原子力研究所研究情報部研究情報課（〒319-1195 茨城県那珂郡東海村）あて、お申し越し下さい。なお、このほかに財団法人原子力弘済会資料センター（〒319-1195 茨城県那珂郡東海村日本原子力研究所内）で複写による実費領布を行っております。

This report is issued irregularly.

Inquiries about availability of the reports should be addressed to Research Information Division, Department of Intellectual Resources, Japan Atomic Energy Research Institute, Tokai-mura, Naka-gun, Ibaraki-ken 319-1195, Japan.

© Japan Atomic Energy Research Institute, 1999

編集兼発行 日本原子力研究所

Neutronics Study on the JAERI 5MW Spallation Neutron Source  
— Neutronic Performance of the Reference Target-moderator-reflector  
System and the Target Shape/Size Effects —

Makoto TESHIGAWARA\*, Noboru WATANABE\*\*, Hiroshi TAKADA,  
Tetsuya KAI, Hiroshi NAKASHIMA, Tadashi NAGAO, Yukio OYAMA,  
Yujiro IKEDA and Kazuaki KOSAKO\*

Center for Neutron Science  
Tokai Research Establishment  
Japan Atomic Energy Research Institute  
Tokai-mura, Naka-gun, Ibaraki-ken

(Received February 3, 1999)

Neutronic performance of slow neutrons from various moderators and nuclear heating in the moderator were studied by computer simulations in the proposed reference target-moderator-reflector system for a 5 MW pulsed spallation neutron source projected in Japan Atomic Energy Research Institute. The performance per MW in the beam power was found to be, at least, comparable or superior to that of other laboratories (SNS, ESS). Our proposed system at 5 MW provides 1.5 times higher time integrated slow neutron intensity and about 80 times higher peak neutron intensity compared with that of existing intense source, ILL.

Target shape/size effects on slow neutron intensity were also studied. This result showed that slow neutron intensities do not strongly depend upon the target shape. This result suggested that more flexible engineer design could be made.

Keywords: Slow Neutron Intensity, Moderator Neutronics, Target-moderator-reflector System, High Power Pulsed Spallation Neutron Source, Time Distribution, Nuclear Heating, Target Shape/Size Effect

---

\* Post-Doctoral Fellow

\*\* Scientific Consultant

\* Sumitomo Atomic Power Industries Ltd.

5MW 核破碎中性子源開発におけるニュートロニクス研究  
—基準ターゲット・モデレータ・反射体における中性子特性及び  
ターゲット形状/サイズのそれに及ぼす影響—

日本原子力研究所東海研究所中性子科学研究センター  
勅使河原 誠\*・渡辺 昇\*\*・高田 弘・甲斐 哲也  
中島 宏・永尾 忠司・大山 幸夫・池田裕二郎  
小迫 和明\*

(1999 年 2 月 3 日受理)

原研中性子科学研究計画で目指す 5MW 短パルス核破碎中性子源で提案されている基準ターゲット・モデレータ・反射体システムの性能評価を行うため、各種モデレータから得られる冷、熱及び熱外中性子強度に関するニュートロニクス計算を行った。陽子ビーム出力 (MW) 当たりの中性子強度は、最も関心の高い冷中性子の場合、他の計画中 (SNS 及び ESS) の同規模の大強度中性子源と比較して高い効率で得られることが分かった。さらに、5MW の出力では、現存する ILL 強力中性子源の時間積分強度で 1.5 倍、ピーク強度で約 80 倍の強度を与える結果となった。

また、基準系に対するターゲット形状/サイズの中性子強度に及ぼす影響を検討した。その結果、ターゲット形状の変化は、特にモデレータの無い方向の増減は、中性子強度に大きな影響を及ぼさないことが示され、ターゲットの工学的な設計上の大きな裕度を与える得ることが明らかとなった。

---

東海研究所:〒319-1195 茨城県那珂郡東海村白方白根2-4

\* 博士研究員

\*\* 特別研究員

\* 住友原子力工業(株)

## Contents

1. Introduction .....	1
2. Model of Reference Target-moderator-reflector System .....	1
3. Calculations .....	2
3.1 Calculational Details .....	2
3.2 Fitting Functions on Energy Spectral Intensity .....	3
4. Neutronic Performance .....	4
4.1 Neutronic Characteristic of Reference Target-moderator-reflector System .....	4
4.1.1 Time Integrated Neutron Intensity .....	4
4.1.2 Time Distribution from Cold Moderator .....	5
4.1.3 Nuclear Heating in Cryogenic Moderator .....	5
4.2 Target Shape/Size Dependence .....	6
4.2.1 Dependence of Target Aspect Ratio .....	6
4.2.2 Dependence of Extended Target Size to Horizontal or Vertical Direction .....	6
5. Conclusions .....	7
References .....	8
Appendix .....	27

## 目 次

1. 概 要 .....	1
2. 基準ターゲット・モデレータ・反射体システムのモデル .....	1
3. 計 算 法 .....	2
3.1 計算条件 .....	2
3.2 中性子強度におけるフィッティング関数 .....	3
4. 中性子特性 .....	4
4.1 基準ターゲット・モデレータ・反射体システムの中性子特性 .....	4
4.1.1 時間積分中性子強度 .....	4
4.1.2 冷中性子の時間スペクトル .....	5
4.1.3 モデレータ中の核発熱 .....	5
4.2 中性子強度のターゲット形状/サイズ依存について .....	6
4.2.1 ターゲット形状扁平度依存性 .....	6
4.2.2 ターゲット形状大きさ依存性（水平方向及び垂直方向） .....	6
5. 結 論 .....	7
参考文献 .....	8
付 録 .....	27

This is a blank page.

## 1. Introduction

We have reported the results for the bare target neutronics on the target system of 5 MW spallation Neutron Source proposed by JAERI<sup>1)</sup>. As pointed out in the report, optimizing target material and shape further needs indispensably, calculations on the full target-moderator-reflector systems. Calculations are essential to maximize the neutronic performance of slow neutrons from the moderators.

In the present study, we calculated energy spectral intensities of slow neutrons and time distributions from various moderators and energy deposition in cryogenic moderators, for full target-moderator-reflector systems.

The main purpose of the present investigation is to obtain the neutronic performance (slow neutron intensity and pulse shape) of the reference target-moderator-reflector system<sup>2)</sup>. We compare the performance of the present results with those obtained at other laboratories or projects in order to evaluate and justify our reference system.

It is another important issue for the target engineering to investigate the effect of the target shape as well as the proton beam footprint on the time-averaged-slow-neutron intensity. At higher beam power target size becomes large compare to an ideal one due to the maximum acceptable beam power density and safety reason (triple target vessel, fourfold cryogenic moderator vessel, etc.). It may lead to a poor neutronic performance. We performed some calculations to investigate such effects and report the results.

## 2. Model of reference target-moderator-reflector system

A target-moderator configuration is illustrated in Fig. 1. The coupling scheme of the target and the moderator is a wing geometry type. The configuration of the target-moderator-reflector system is illustrated in Fig. 2.

Table 1 shows the proton beam, target and reflector parameters. The combinations of the main parameters of the proton beam, the target and the reflector examined in this study are summarized in table 2. The proton-current-density profile is assumed to be a rectangular (flat distribution) with a maximum acceptable density of  $48 \mu\text{A}/\text{cm}^2$  at beam power of 5 MW. A rectangular target with a hemispherical shape beam window is adopted to obtain a good neutronic performance. Lateral target dimensions are assumed to be beam height plus 3 cm in vertical direction and beam width plus 4 cm in horizontal direction in the reference system. The target material is contained by a double stainless steel vessel (SUS316). It is filled with water between double SUS316 structures.

Two coupled hydrogen (liquid or supercritical at 20 K) moderators with water premoderators (PM) at ambient temperature (hereafter we call coupled  $\text{H}_2$  moderator) are located above the target to realize the highest peak intensity together with the highest time-integrated intensity.

The coupled  $H_2$  moderator has dimensions of  $12 \times 12 \times 5 \text{ cm}^3$ . The ortho / para ratio of hydrogen at 20 K in the reference system is assumed to be 75% / 25% (normal hydrogen). Two hydrogen moderators share the backside with PM.

One high-resolution thermal neutron moderator (upstream) and one high-resolution epithermal neutron moderator (downstream) are located below the target as shown in Fig. 3<sup>2)</sup>. The latter consists of light water at ambient temperature. Two high resolution moderators below the target are decoupled. The dimensions are  $10 \times 10 \times 5 \text{ cm}^3$  for the thermal moderator and  $10 \times 10 \times 3 \text{ cm}^3$  for the epithermal moderator. Each moderator has open angle of  $50^\circ$  and  $10 \times 10 \text{ cm}^2$  of viewed surface for neutron beam extraction. In the calculation a 3 mm-thick  $B_4C$  decoupler is used. The neutron cut-off energy is tentatively fixed at 1 eV by changing the number of  $B_4C$ . The material of a cryogenic moderator for a high resolution thermal neutron source has not specified yet in the reference system, and therefore we tentatively put a decoupled liquid-methane ( $L\text{-CH}_4$ ) moderator at the position of the upstream moderator below the target. The main parameters of the moderators investigated are summarized in Table 3.

We assume that two reflectors of Lead (Pb) and Beryllium (Be) as a reference size ( $80^W \times 160^H \times 120^L \text{ cm}^3$ ). Each reflector has neutron-beam extraction holes from moderators as shown in Fig. 3.

We performed extensive calculations for various combinations of proton beam-target-reflector parameters as shown in Table 2 to compare the neutronic performance with that of the reference model.

Details of the calculational model of the reference target-moderator-reflector system are described in Appendix.

### 3. Calculations

#### 3.1 Calculational details

In order to predict the neutronic performance of each moderator in the reference system, especially on the spectral intensity and pulse shapes, and to provide basic data for a moderator engineering such as nuclear heating in moderators, we performed neutronic calculations using a code system which consists of NMTC/JAERI<sup>3-4)</sup> and MCNP-4A<sup>5)</sup>. NMTC/JAERI solves the high energy hadron transport (above 20 MeV) and MCNP-4A does the neutron transport below 20 MeV with cross section libraries, FSXLIB-JEFF, FSXLIB-JFNS and THERXS. The energy bins used in the present calculations are shown in Fig. 4. The total number of the energy bins was 156 including 82 below 1 eV. For a mercury (Hg) target, cross sections evaluated recently at JAERI were used<sup>6)</sup>. The total number of protons incident upon the target to produce neutrons was about  $3 \times 10^7$  in each NMTC/JAERI Monte Carlo simulation. The number of neutrons from the target in MCNP-4A calculations was determined so that the maximum statistical error of neutron in-



tensity per unit energy bin at the Maxwellian peak of thermalized neutrons is less than 1%. Point detector estimators to obtain the neutron intensity were located at 2 m from the moderator viewed surface.

### 3.2 Fitting functions on energy spectral intensity

Figure 5 shows the typical calculated spectral intensities (histogram) of neutrons from the different moderators at the reference system with a Hg target - Pb reflector combination. The calculated values of the spectral intensities from moderators were fitted by using a semi-empirical formula<sup>7)</sup> described below.

The leakage slow neutron spectrum from a moderator,  $\phi(E)$ , can be expressed as,

$$\phi(E) = \frac{\Phi_{4\pi}(E)}{4\pi} = \frac{J(E, r)}{S d\Omega} = \frac{J(E, r)}{S \left(\frac{1}{r^2}\right)} \quad (1),$$

where  $\Phi_{4\pi}(E)$  is  $4\pi$  equivalent time-averaged-neutron-spectrum.  $J(E, r)$  is neutron spectral intensity given by Monte Carlo simulation at distance,  $r$ , from the moderator surface and  $S$  is viewed surface area for neutron beam extraction from the moderator.

In the case of a coupled  $H_2$  moderator,  $\phi(E)$  can be expressed as a sum of the thermal equilibrium spectrum,  $\phi_{th}(E)$  (Maxwellian), and epithermal spectrum in the slowing down region,  $\phi_{epi}(E)$  ( $1/E$  spectrum),

$$\phi(E) = \phi_{th}(E) + \theta_{cur}(E) \phi_{epi}(E) \quad (2),$$

where the parameter  $\theta_{cur}(E)$  is an appropriate joining function as described later. The spectrum  $\phi_{th}(E)$  can be expressed as,

$$\phi_{th}(E) = J \frac{E}{E_T^2} e^{-E/E_T} \quad (3),$$

where  $E_T$  is the characteristic energy of the Maxwellian portion of the spectrum and  $J$  is the energy integrated intensity of Maxwellian part of spectrum.  $\phi_{epi}(E)$  is expressed as,

$$\phi_{epi}(E) = \rho(E) \frac{\phi_{1eV}}{E} \left( \frac{E}{1eV} \right)^\alpha \quad (4),$$

where  $\phi_{1eV}$  represents the intensity of slowing down neutron at 1 eV and  $\alpha$  is a constant between 0 and 0.2.  $\rho(E)$  is given by,

$$\rho(E) = 1 + \delta e^{-y} (1 + y + 0.5 y^2) \quad (5),$$

where  $y = 0$  for  $E < E_p$

$$y = \gamma (E - E_p) \quad \text{for } E \geq E_p ,$$

$\delta$ ,  $\gamma$  and  $E_p$  are the fitting parameters.

The joining function  $\theta_{cut}(E)$  is given by,

$$\theta_{cut}(E) = 1 - e^{-x}(1 + x + 0.5 x^2) \quad (6) ,$$

where  $x = 0$  for  $E < E_{cut}$  ,

$$x = \beta (E - E_{cut}) \quad \text{for } E \geq E_{cut} ,$$

and  $\beta$  and  $E_{cut}$  are also the fitting parameters.

In the case of the decoupled L-CH<sub>4</sub> and water moderator, a neutron spectrum  $\phi(E)$  can also be expressed as a sum of  $\phi_{th}(E)$  (Maxwellian) and  $\phi_{epi}(E)$  (1/E spectrum) by using another semi-empirical formula ,

$$\phi(E) = \phi_{th}(E) + \Delta(E) \phi_{epi}(E) \quad (7) ,$$

where  $\Delta(E)$  is an appropriate joining function.  $\phi_{th}(E)$  and  $\phi_{epi}(E)$  can be expressed as,

$$\phi_{th}(E) = J \frac{E}{E_T^2} e^{-E/E_T} \quad (8) ,$$

$$\phi_{epi}(E) = \phi_{lev} \frac{1}{E} \left( \frac{E}{1 \text{ eV}} \right)^\alpha \quad (9) .$$

The joining function,  $\Delta(E)$  , is given by,

$$\Delta(E) = \frac{1}{1 + \exp\left(\frac{a}{\sqrt{E}} - b\right)} \quad (10) ,$$

where  $a$  and  $b$  are the fitting parameters.

Figure 6 shows an example of the fitted spectral intensities of neutrons,  $\phi(E)$  , per unit proton beam power (MW) with the calculated histograms from three different moderators.

## 4 Neutronic performance

### 4.1 Neutronic characteristic of reference target-moderator-reflector system

#### 4.1.1 Time integrated neutron intensity

The spectral intensities obtained by using fitting functions for the reference system (a Hg target and Pb reflector) are compared in Fig. 7 with those studied in other laboratories (a coupled H<sub>2</sub> moderator without PM for the LANSCE Upgrade project<sup>8)</sup> and cold second neutron source (CSN2) at the Institute Laue Langevin (ILL) in Grenoble<sup>9)</sup>). The main parameters,  $J$ ,  $E_T$  and  $\phi_{lev}$  characterize the spectral intensities from a moderator, as described in section 3.2. Those results

for two reflectors of Pb and Be are summarized in Tables 4-6, compared with results obtained by other laboratories<sup>8 and 10-12</sup>). The observations from the results on the time integrated intensities from the coupled H<sub>2</sub> moderators for the reference system are summarized as follows:

(1) The cold neutron intensity is superior to that of ILL, which has the highest cold neutron intensity in the world if feasible to develop neutron source of more than 4 MW by spallation source as shown in Fig. 7. The spectral intensities at the Maxwellian peak or the time-integrated cold-neutron-intensity J per MW of the present model are at least comparable or more than those of LANSCE upgrade project as shown in Table 4.

(2) The slowing-down neutron intensities at 1 eV from the coupled H<sub>2</sub> moderator above the target are almost the same as those obtained by other laboratories (LANSCE Upgrade, SNS and IPNS Upgrade).

(3) The Be reflector gives a higher cold neutron intensity by about 45 % and lower energy deposition in the moderator which is shown below than the Pb one. The former, however, provides a poor pulse structure compared with the latter as shown in section 4.1.2. Thus, selection of reflector material gives a critical effect not only on neutronic performance but also on the overall system performance.

(4) The cold neutron intensities from the coupled H<sub>2</sub> moderator are about a factor of 4 times higher than that from the decoupled L-CH<sub>4</sub> moderator (as a reference) as summarized in Tables 4 and 5.

(5) The cold neutron intensities from the two coupled H<sub>2</sub> moderators are almost the same. This shows that both moderators take the first seat for neutron intensity i.e., it has considerably good coupling efficiency of target and moderators.

These results justify the presently summarized concept of reference target-moderator-reflector system as far as the neutronic performance is concerned.

#### 4.1.2 Time distribution from cold moderator

Time distributions (pulse shapes) of neutrons from the cold moderator at 2.0-2.2 meV are shown in Fig. 8. Both reflectors (Pb and Be) gives almost the same peak neutron intensity, while the Pb reflector provides a narrower pulse width than the Be one. The predicted cold neutron peak intensity is at least 80 times higher than that of ILL. To obtain further higher intensity, we propose a fully extended PM concept and further optimization study is continued.

#### 4.1.3 Nuclear heating in cryogenic moderator

The nuclear heating in a cryogenic moderator is one of the most important technical issues in the design study of an intense spallation source. We calculated the energy deposition in the cryogenic moderators (a coupled H<sub>2</sub> moderator, L-CH<sub>4</sub> and a simple H<sub>2</sub> etc.). The results are

summarized in Table 7 and spatial distributions are compared in Fig. 9. The use of PM in a coupled  $H_2$  moderator reduces the energy deposition by about 50 % but energy depositions are still very high. A Be reflector can provide a higher integrated intensity (J) with a longer tailed time distribution, described above, and reduce the energy deposition by about 35 % to compared with the Pb one. However the reduction rate at the hottest region close to the target is rather small as seen in Fig. 9.

The candidate moderator of high resolution thermal moderator is decoupled poisoned L- $H_2$ . The energy deposition in the moderator is further higher than that of coupled  $H_2$  one as shown in Fig. 9.

## 4.2 Target shape/size dependence

We performed neutronic calculations concerning the effects of target shape and size on the spectral intensity of slow neutrons. We consider two points; one is changing a target aspect ratio ( $b/a$ , where  $a$  and  $b$  are the horizontal and the vertical beam sizes, respectively) and the other is extending a target size to horizontal or vertical direction of the target with a constant proton beam cross section. The latter case provides the important information for target engineering rather than neutronic performance.

### 4.2.1 Dependence of target aspect ratio

Figure 10 shows time-integrated-slow-neutron intensities,  $J$ , and  $\phi_{1eV}$  for various moderators as a function of the target aspect ratio. The target sizes and shapes are automatically defined from each aspect ratio. The data indicated by closed triangles are for a reduced beam current density (two third of  $48 \mu A/cm^2$ ), which corresponds to a larger beam size, accordingly a larger target size. The results indicate that the slow neutron intensities,  $J$  and  $\phi_{1eV}$  are insensitive to the target aspect ratio and a somewhat increase of target size. This fact will provide a larger flexibility for the target engineering rather than for the neutronic performance.

### 4.2.2 Dependence of extended target size to horizontal or vertical direction

Figure 11 shows time-integrated-slow-neutron intensity dependence of extended target size to horizontal direction. The slow neutron intensities are slightly reduced according to extension of the target to horizontal direction. It was worried that it would reduce the neutronic performance because a certain-sized flowing duct to horizontal direction of the target in a wing geometry is needed. This result is “glad tidings” for the target development engineering.

On the other hand, Figure 12 shows its intensity dependence of extended target size to vertical direction. The neutron intensity decreases considerably compared to that of horizontal

extension case. This is simply because of increase in the distance between target and moderator (vertical direction). As the reference, the results of void and reduced proton current density cases also are shown in Fig. 12. In the void case, the extended vertical region is filled with not Hg but vacuum. If a target size (distance between moderator and target) inevitably becomes larger due to acceptable beam power density, safety vessel (target and moderator), etc., this result shows that it leads a poor neutronic performance.

Figure 13 compares the effect of target size on the neutron intensity,  $\phi_{lev}$  from decoupled water moderators of different target-moderator combination. These results provide an important information of target-moderator coupling efficiency. The present system (the wing geometry type) combined with a flatter target and a moderator gives higher neutron intensities,  $\phi_{lev}$  compared with the ESS model<sup>13)</sup> (wing and flux trap geometry type) combined with split (cylindrical) target and moderator as shown in Fig. 13. This is mainly due to a larger high luminosity region by the flatter target and high efficient combination of target-moderator in our model. Target size effect on a neutron intensity is similar to that of flux trap geometry type rather than wing type in the ESS model.

## 5. Conclusions

From the results of present calculations, the followings are concluded:

(1) It is confirmed that the neutronic performance based on the present concept is at least comparable or superior to those predicted for other intense pulsed spallation neutron source projects. The time-integrated cold neutron intensity at 5 MW is estimated to be about 1.5 times higher than that of an existing intense cold source, ILL. Thus it can be said that the proposed concept of the target-moderator-reflector system is attractive.

(2) Although a Be reflector gives a wider neutron pulse from the coupled H<sub>2</sub> moderator than a Pb one, the former gives a higher intensity by about 45 % than the latter and reduces the energy deposition in the moderator. However, the energy deposition at the hottest region by both reflectors is high. How to mitigate the energy deposition in cryogenic moderator is also key issue for target development.

(3) Slow neutron intensities are insensitive to the target shape/size (aspect ratio and extended target size to horizontal). These results make target engineering more flexible, which encourage the target development.

We obtained useful information for development of intense spallation source. There are still many engineering issue to be solved such as the heat removable in cryogenic moderator and pressure wave in the target, etc., however.

## References

- 1) M. Teshigawara, N. Watanabe, H. Takada, H. Nakashima, T. Nagao, Y. Oyama and K. Kosako : “Neutronic studies of bare targets for JAERI Pulsed Spallation Neutron Source”, JAERI-Research 99-010
- 2) N. Watanabe, M. Teshigawara, K. Aizawa, J. Suzuki and Y. Oyama : “A target-moderator-reflector concept of the JAERI 5 MW pulsed spallation neutron source”, JAERI-Tech 98-011 (1998).
- 3) Y. Nakahara and T. Tsutsui : “NMTC/JAERI, A Code System for High Energy Nuclear Reactions and Nucleon-Meson Transport Code”, JAERI-M 82-198 (1982) (in Japanese).
- 4) H. Takada, N. Yoshizawa, K. Kosako and K. Ishibashi : “An Upgrade Version of Nuclear Meson Transport Code NMTC / JAERI - 97, JAERI - Code”, JAERI-Data/Code 98-005 (1998).
- 5) J. F. Briesmeister (Ed.) : “MCNP, A General Monte Carlo N-Particle Transport Code, Version 4A”, LA-12625 (1993).
- 6) K. Shibata, T. Fukahori, S. Chiba and N. Yamamuro : J. Nucl. Sci. Tech., 34, 1171 (1997).
- 7) J. M. Carpenter, R. A. Robinson, A. D. Talor and D. J. Picton : Nucl. Instrum. Method., A234, 542 (1985).
- 8) P. D. Ferguson, G. J. Russel and E. J. Pitcher : “Reference moderator calculated performance for the LANSCE Upgrade project”, Proc. 13th Meeting Int. Collaboration on Advanced Neutron Sources (PSI, Switzerland, Oct. 11-14, 1995) 510
- 9) P. Ageron : Nucl. Instr. and Meth., A284, 197 (1989).
- 10) ORNL : “National Spallation Neutron Source Conceptual Design Report Vol. 1”, Chapter 5 TARGET SYSTEMS, NSNS/CDR-2/V1 (1997).
- 11) ANL : “IPNS Upgrade: A Feasibility Study”, Chapter IV (TARGET STATIONS), ANL/95/13 (1995).
- 12) N. Watanabe : “R&D of neutron beam using nuclear spallation”, Genshikaku Kenkyu, 40, 71 (1995) (in Japanese).
- 13) D. J. Picton, T. D. Beynon and T. A. Broome : “Neutronics studies for the ESS SOURCE”, Proc. 13th Meeting Int. Collaboration on Advanced Neutron Sources (PSI, Switzerland, Oct. 11-14, 1995) 522

Table 1 Specification of proton beam, target and reflector

Proton			
Energy (GeV)	Profile	Current density ( $\mu\text{A}/\text{cm}^2$ )	Beam power (MW)
1.5	Uniform distribution	48	5
Target			
Material	Shape		
Hg	Rectangular		
Reflector			
Material	Size (W x H x L cm <sup>3</sup> )		
Pb or Be	80 x 160 x 120		

Table 2 Combinations of proton beam, target and reflector for the study of target shape/size effects

Aspect ratio dependence			
Aspect ratio (b/a)	Proton Beam size (a x b $\text{cm}^2$ )	Target Size (W x H $\text{cm}^2$ )	Reflector Material
0.688	10 x 6.88	14 x 9.88	Pb or Be
<b>0.387</b>	<b>13.35 x 5.16</b>	<b>17.35 x 8.16</b>	<b>Pb or Be</b>
0.172	20 x 3.44	24 x 6.44	Pb or Be
Dependence of horizontal extended			
	Proton Beam size (a x b $\text{cm}^2$ )	Target Size	Reflector Material
	13.35 x 5.16	27.35 x 8.16	Pb
	13.35 x 5.16	37.35 x 8.16	Pb
Dependence of vertical extended			
	Proton Beam size (a x b $\text{cm}^2$ )	Target Size	Reflector Material
	13.35 x 5.16	17.35 x 11.16*	Pb
	13.35 x 5.16	17.35 x 13.32	Pb
	13.35 x 10.32**	17.35 x 13.32	Pb
	13.35 x 5.16	17.35 x 18.48	Pb
	13.35 x 15.48***	17.35 x 18.48	Pb

**0.387** : This color shows reference system.

\*Two cases were studied ( Void case and filled with Hg case).

\*\* Reduced current density case :  $48 \times (1/2) \mu\text{A}/\text{cm}^2$

\*\*\* Reduced current density case :  $48 \times (1/3) \mu\text{A}/\text{cm}^2$

Table 3 Moderators for calculational model

Purpose	Cold neutron		Thermal neutron		Epithermal neutron	
	High resolution & high intensity		High resolution		High resolution	
Main moderator	L-H <sub>2</sub> (normal)		Poisoned L-H <sub>2</sub> , L-H <sub>2</sub> +ZrH <sub>2</sub> or a mixed mod. of (S-CH <sub>4</sub> or S-H <sub>2</sub> O) particles + L-H <sub>2</sub>		H <sub>2</sub> O	
size (cm)	12 x 12x 5		10 x 10 x 5*		10 x 10 x 3	
Moderator temp.(K)	20		20		Room temp.	
Premoderator	H <sub>2</sub> O (2.5 cm thick)		Non		Non	
Coupling	Coupled		Decoupled**		Decoupled**	
Cut - off energy (eV)	--		1		1	
Angular coverage / viewed surface	50°		50°		50°	
No. of viewed surface	1		2		2	
No. of moderators	2		1		1	

\*The candidate of this moderator is Poisoned L-H<sub>2</sub>, L-H<sub>2</sub>+ZrH<sub>2</sub> or (S-CH<sub>4</sub> or S-H<sub>2</sub>O) particles +L-H<sub>2</sub> but we have not decided it. Decoupled liquid CH<sub>4</sub> at 100 K was put at this point in the present calculation as a reference cold moderator for comparison with the coupled moderators above target.

\*\*Decoupler is B<sub>4</sub>C of thickness of 3 mm.Cut - off energy was controlled by changing the number density of B<sub>4</sub>C.



Table 4 Calculated results for coupled H<sub>2</sub> moderators

Facility	Target /Reflector	Material /Coupling	J (n/cm <sup>2</sup> /s/sr/MW) x10 <sup>11</sup>	Er (meV)	Integrated intensity (E < 0.4 eV) x 10 <sup>13</sup> (n/cm <sup>2</sup> /s/MW)	$\phi_{\text{eV}}$ (n/cm <sup>2</sup> /s/sr/eV/MW) x10 <sup>11</sup>	Integrated intensity (0.4 eV < E < 0.1 MeV) x 10 <sup>13</sup> (n/cm <sup>2</sup> /s/MW)	
JAERI	Hg/Pb	H2/Coupled	33.0	3.6	7.9	4.6	7.3	Forward
JAERI	Hg/Pb	H2/Coupled	32.6	3.7	7.5	4.1	6.5	Backward
JAERI	Hg/Be	H2/Coupled	50.1	3.6	10.4	3.6	4.9	Forward
JAERI	Hg/Be	H2/Coupled	45.4	3.6	9.7	3.4	4.6	Backward
LANSCE	W(D2O)/Be	H2/Coupled	36.0	3.6		3.3		
LANSCE	W(D2O)/Be	H2/Decoupled	7.5	3.1		3.1		
SNS	Hg/Ni	H2/Decoupled				2.7		
IPNS- Upgrade	Ta/Be	H2/Coupled				4.7		Down stream

Table 5 Calculated results for cryogenic moderators (L-CH<sub>4</sub>)

Facility	Target /Reflector	Material /Coupling	J (n/cm <sup>2</sup> /s/sr/MW) x10 <sup>11</sup>	Er (meV)	Integrated intensity (E < 0.4 eV) x 10 <sup>13</sup> (n/cm <sup>2</sup> /s/MW)	$\phi_{\text{eV}}$ (n/cm <sup>2</sup> /s/sr/eV/MW) x10 <sup>11</sup>	Integrated intensity (0.4 eV < E < 0.1 MeV) x 10 <sup>13</sup> (n/cm <sup>2</sup> /s/MW)	
JAERI	Hg/Pb	L-CH4/Decoupled	8.0	12.7	1.5	2.8	7.8	Right
JAERI	Hg/Pb	L-CH4/Decoupled	8.2	12.4	1.5	2.9	7.8	Left
JAERI	Hg/Be	L-CH4/Decoupled	8.8	12.3	1.7	3.2	6.9	Right
JAERI	Hg/Be	L-CH4/Decoupled	8.9	13.0	1.7	2.9	6.6	Left

Table 6 Calculated results for H<sub>2</sub>O moderators

Facility	Target /Reflector	Material /Coupling	J $\times 10^{11}$ (n/cm <sup>2</sup> /s/MW)	E <sub>T</sub> (meV)	Integrated intensity (E < 0.4 eV) $\times 10^{13}$ (n/cm <sup>2</sup> /s/MW)	$\phi_{\text{eV}}$ (n/cm <sup>2</sup> /s/sr/eV/MW)	Integrated intensity (0.4 eV < E < 0.1 MeV) $\times 10^{13}$ (n/cm <sup>2</sup> /s/MW)	
JAERI	Hg/Pb	H <sub>2</sub> O/Decoupled	10.1	36.2	1.5	2.9	8.8	Forward
JAERI	Hg/Pb	H <sub>2</sub> O/Decoupled	10.1	34.6	1.5	2.7	9.1	Backward
JAERI	Hg/Be	H <sub>2</sub> O/Decoupled	11.3	37.3	1.7	2.9	7.2	Forward
JAERI	Hg/Be	H <sub>2</sub> O/Decoupled	11.7	36.6	1.7	3.0	7.7	Backward
LANSCE	W(D2O)/Be	H <sub>2</sub> O/Decoupled	9.1	30.0		4.0		High-intensity
LANSCE	W(D2O)/Be	H <sub>2</sub> O/Decoupled	2.4	28.0		2.9		High-resolution
LANSCE	W(D2O)/Be	H <sub>2</sub> O/Coupled	66.3	27.0		4.0		
ESS	Hg/Pb	H <sub>2</sub> O/Coupled			3.0		4.9	*
ESS	Hg/Be	H <sub>2</sub> O/Coupled			6.0		5.6	*
ESS	Hg/Pb	H <sub>2</sub> O/Coupled			14.2			**
ESS	Hg/Be	H <sub>2</sub> O/Coupled			15.7			**
KENS	U	H <sub>2</sub> O/Coupled	33.4			12.8		
IPNS Upgrade	Ta/W	H <sub>2</sub> O/Decoupled				2.4		Upstream

\* Reflector size : 60 x 60 x 80 cm<sup>3</sup>\*\* Reflector size : 150 x 150 x 150 cm<sup>3</sup>

Table 7 Total energy deposition in moderator for reference system

Moderator	Coupling	Reflector	Volume (liter)	Average power density (kW/liter)	Total energy deposition (kW)
Coupled H <sub>2</sub>	Coupled	Pb	0.72	3.92	2.82
L-CH <sub>4</sub>	Decoupled	Pb	0.5	11.66	5.83
H <sub>2</sub> O	Decoupled	Pb	0.3	15.77	4.73
L-H <sub>2</sub>	Decoupled	Pb	0.5	7.98	3.99
Coupled H <sub>2</sub>	Coupled	Be	0.72	2.89	2.08
L-CH <sub>4</sub>	Decoupled	Be	0.5	9.47	4.73
H <sub>2</sub> O	Decoupled	Be	0.3	13.00	3.90
L-H <sub>2</sub>	Decoupled	Be	0.5	6.48	3.24

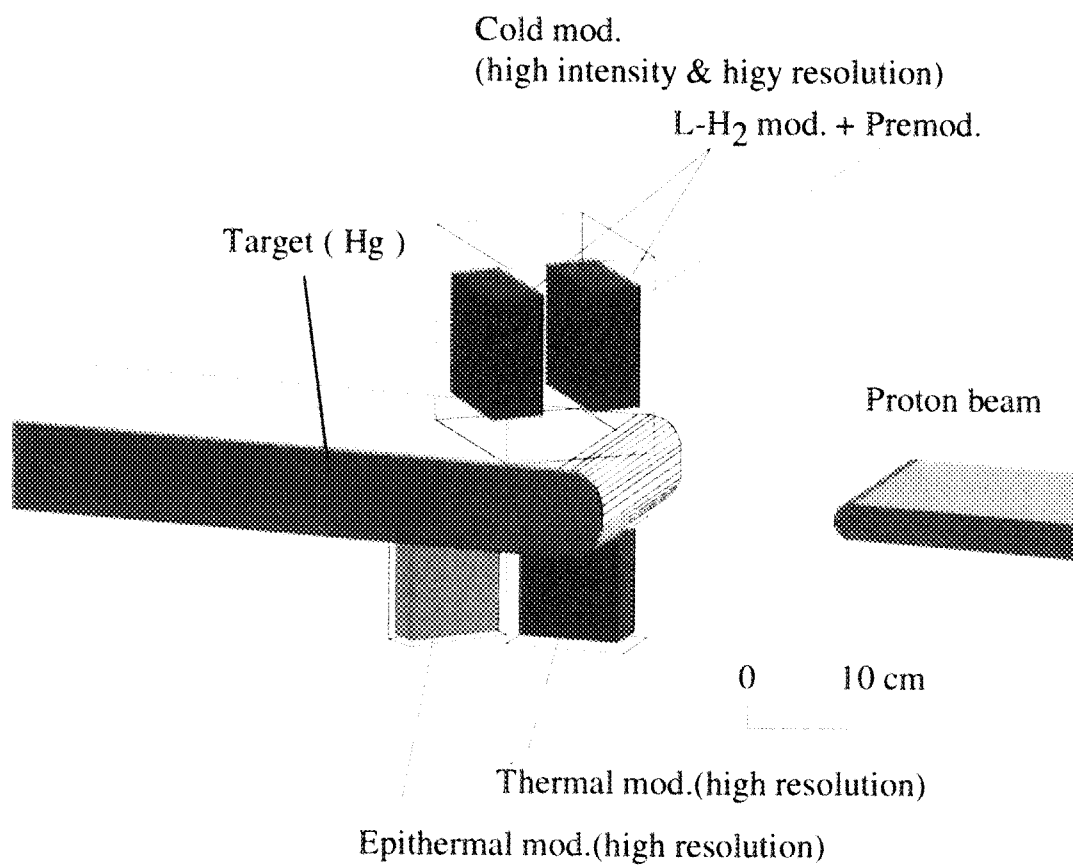


Fig. 1 Layout of target and moderator

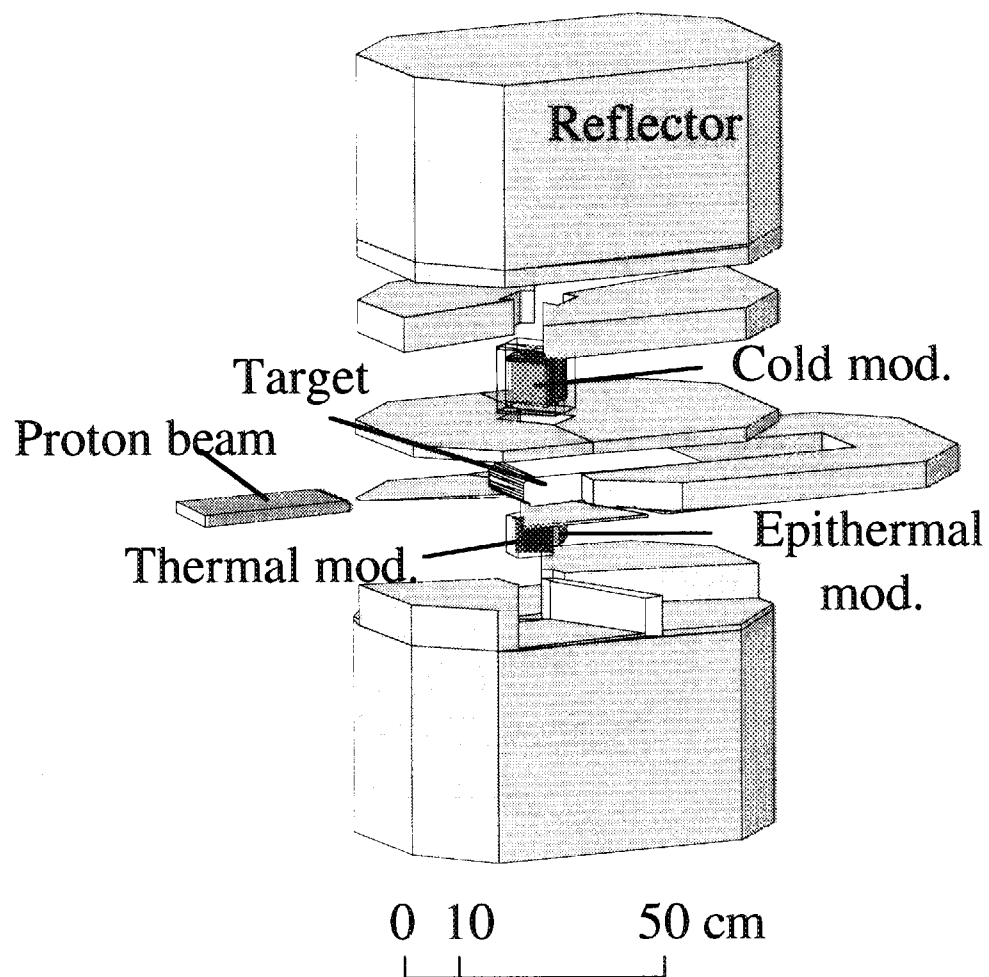


Fig. 2 Illustration of reference target-moderator-reflector assembly

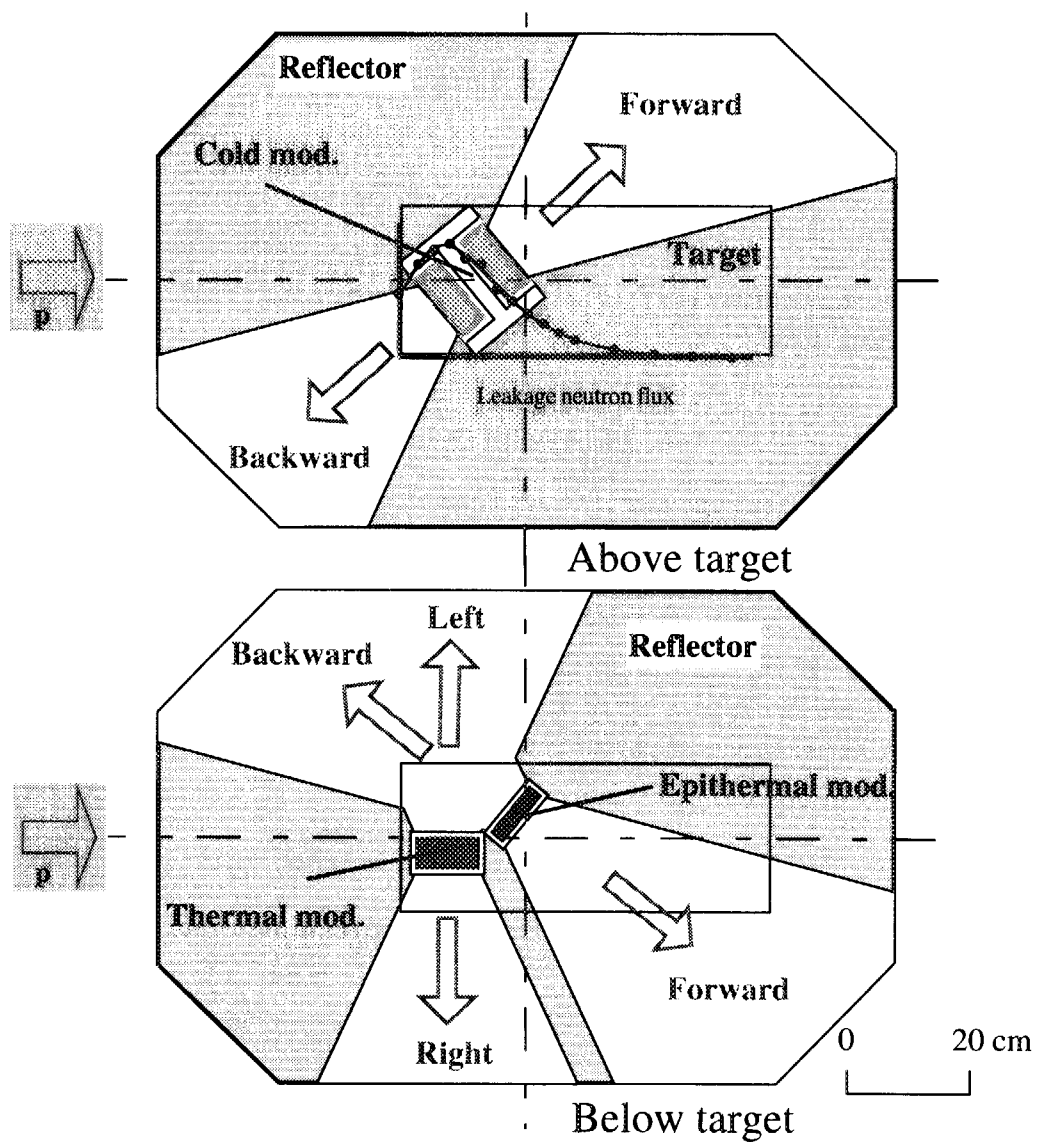


Fig. 3 Calculational model of target-moderator-reflector system

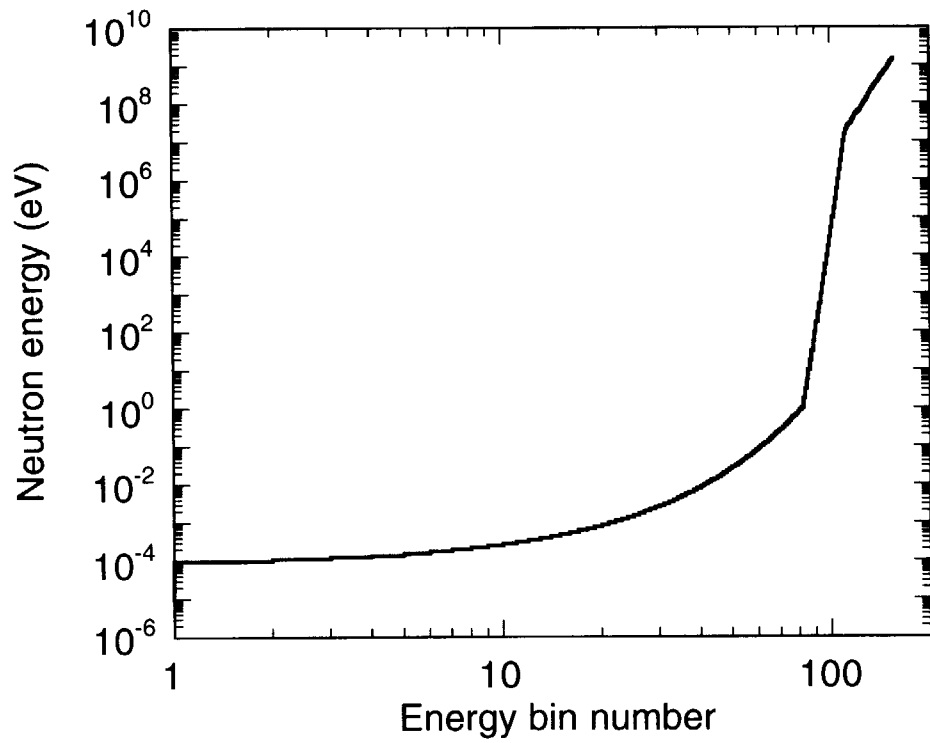


Fig. 4 Relation of energy group and energy bin number

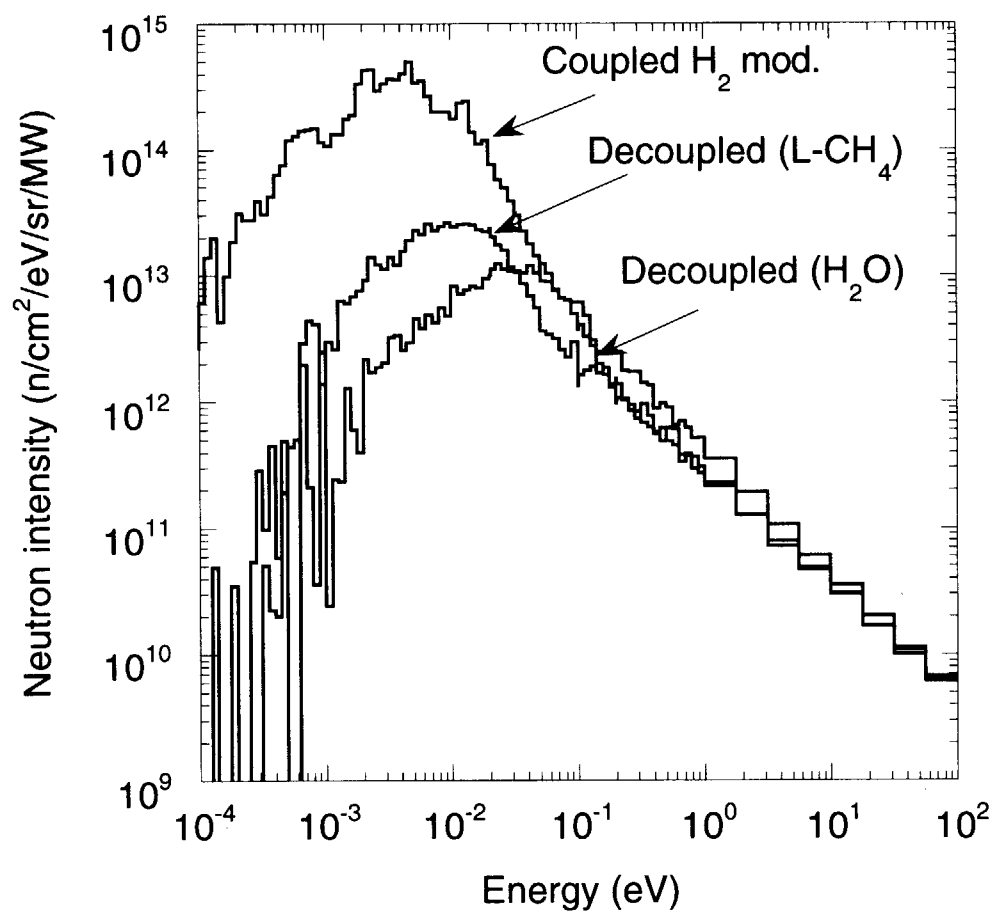


Fig. 5 Histograms of calculated slow-neutron energy spectra from various moderators



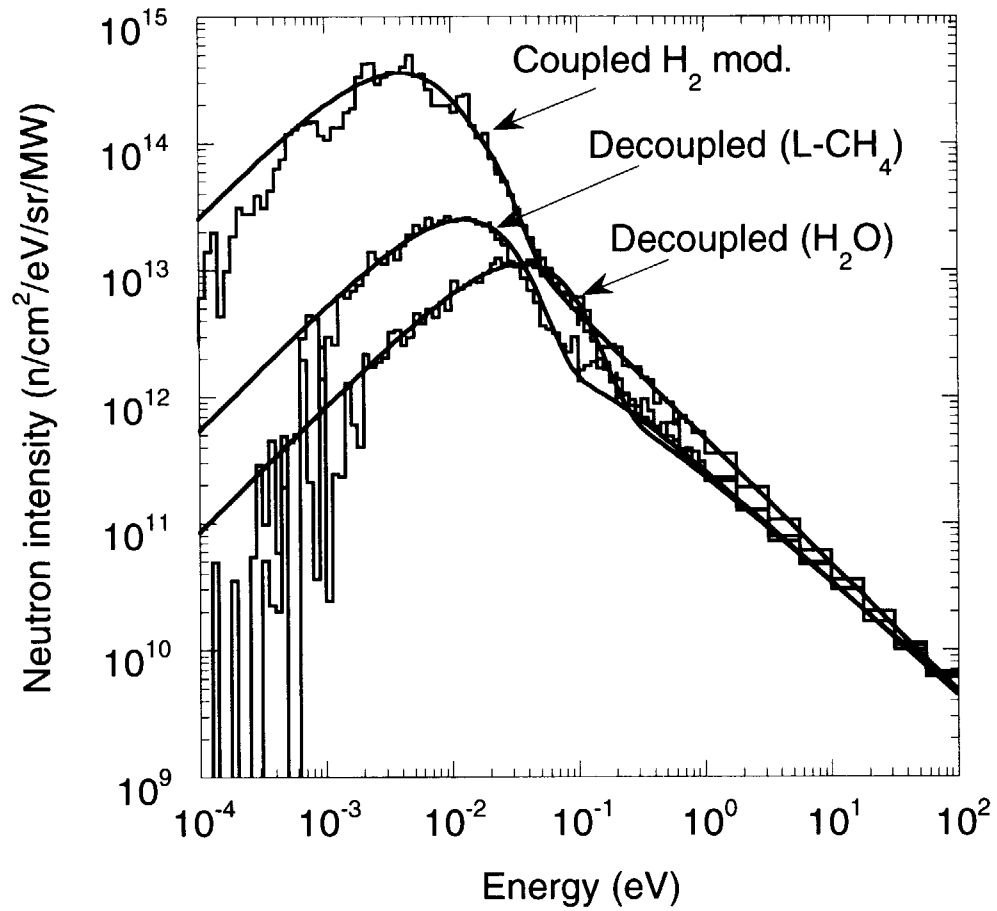


Fig. 6 Curve fit results of spectral intensities from various moderators

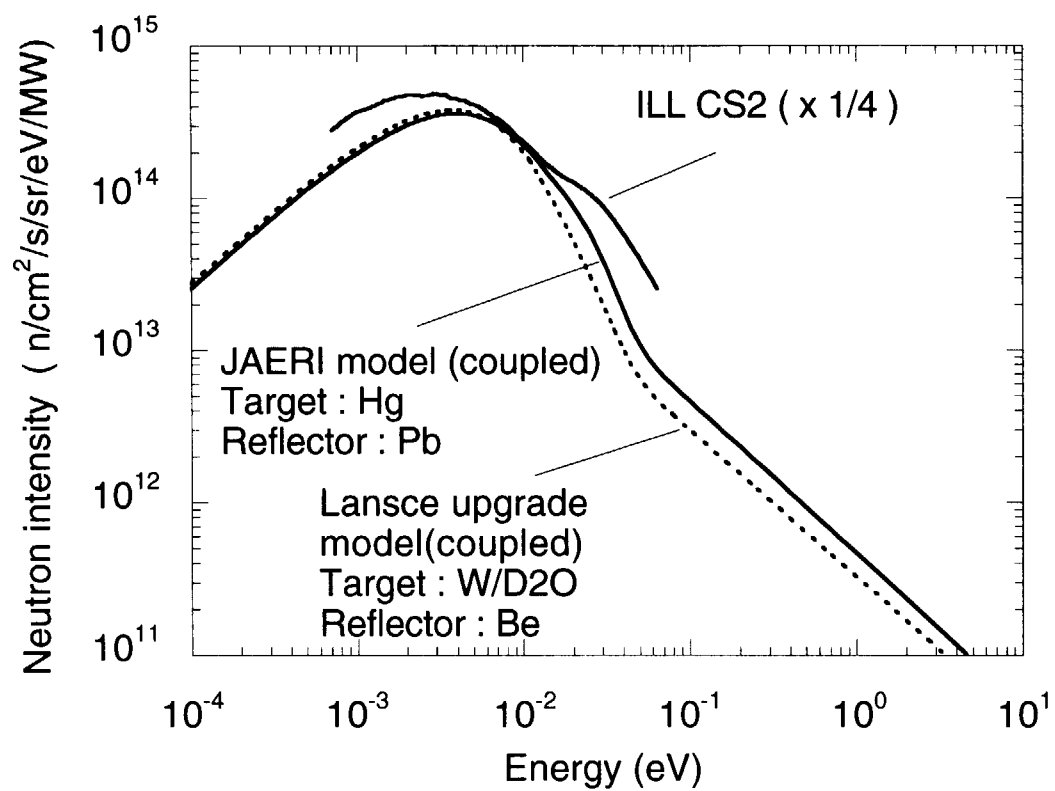


Fig. 7 Neutron spectral intensities from the moderator

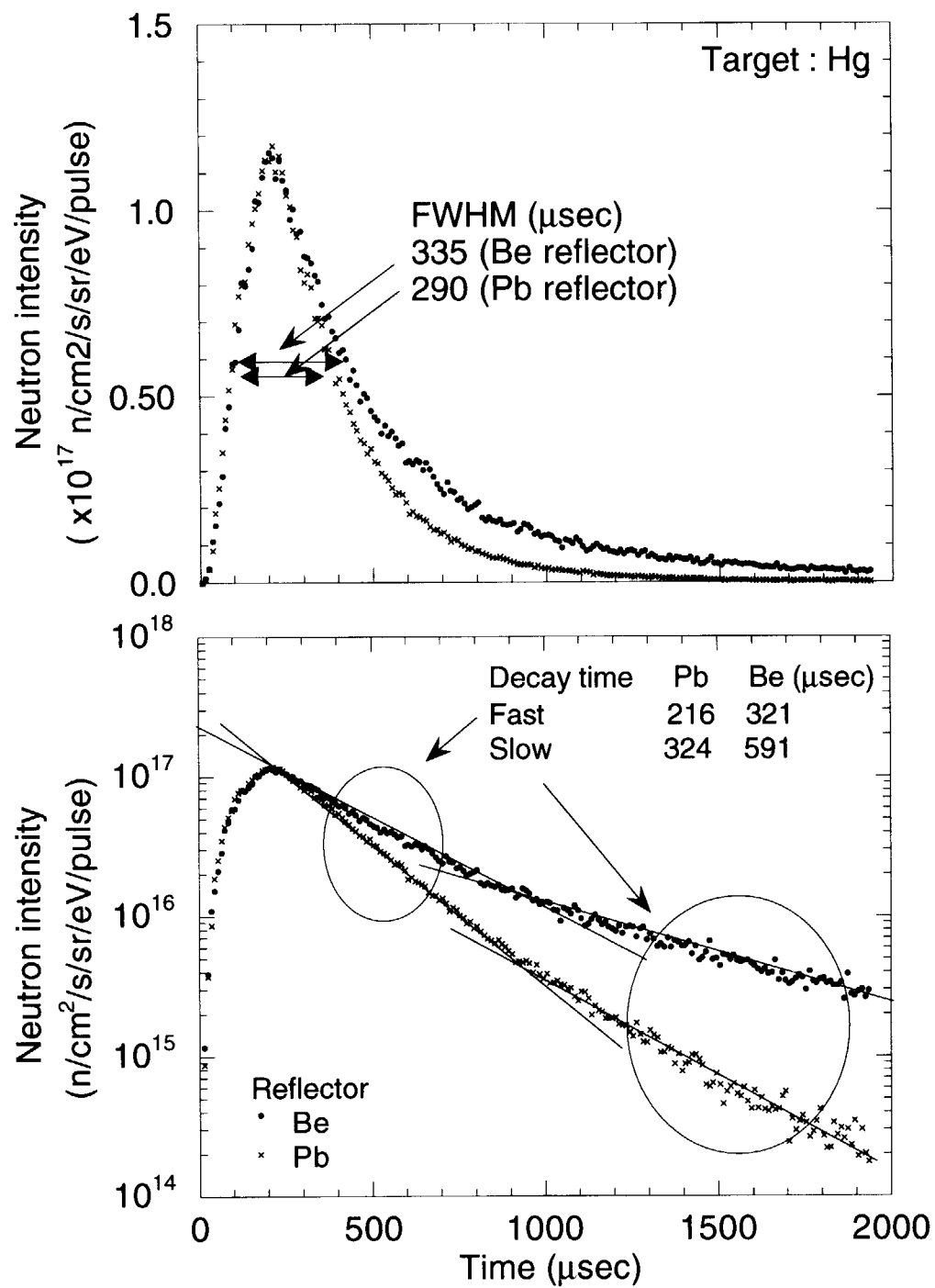


Fig. 8 Time distributions ( $E=2.1$  meV) from coupled  $H_2$  moderator

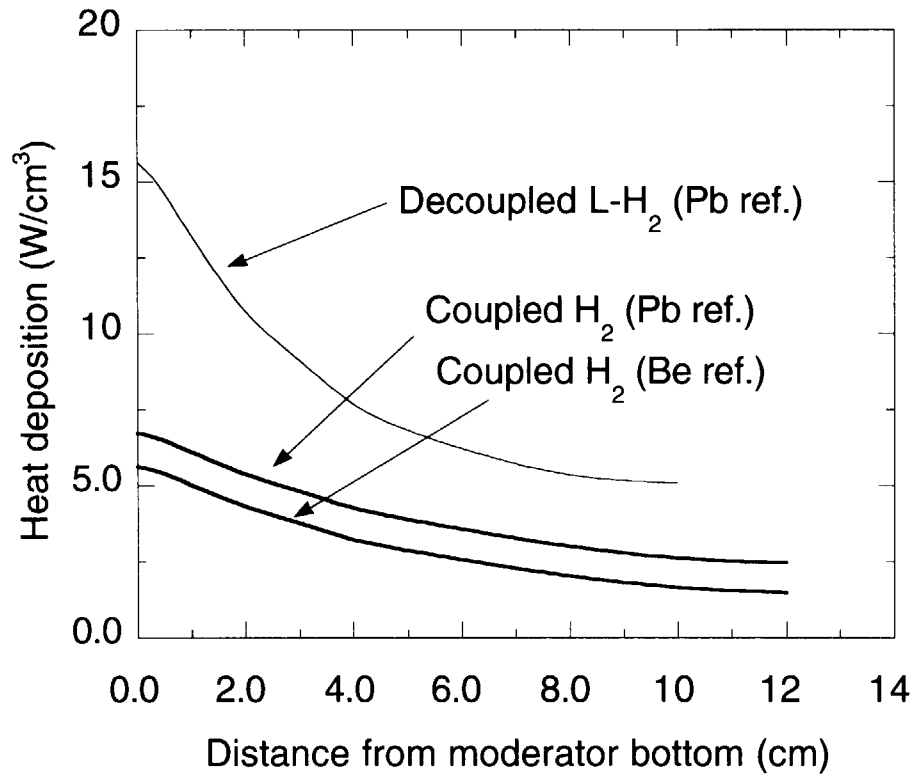


Fig. 9 Spatial distributions of heat deposition in cryogenic moderator as a function of distance from moderator bottom

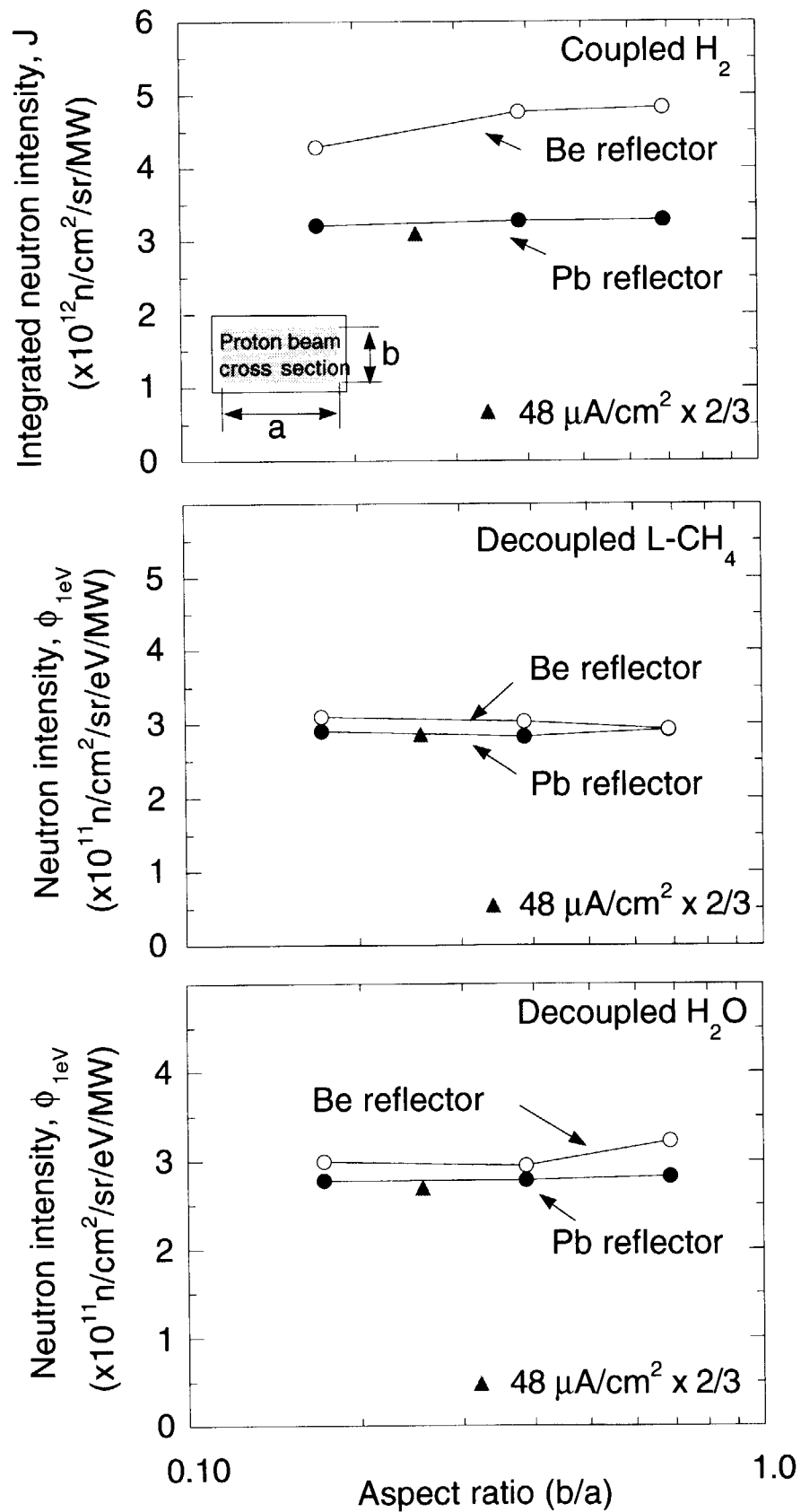


Fig. 10 Beam aspect-ratio dependence of neutron intensity from various moderators

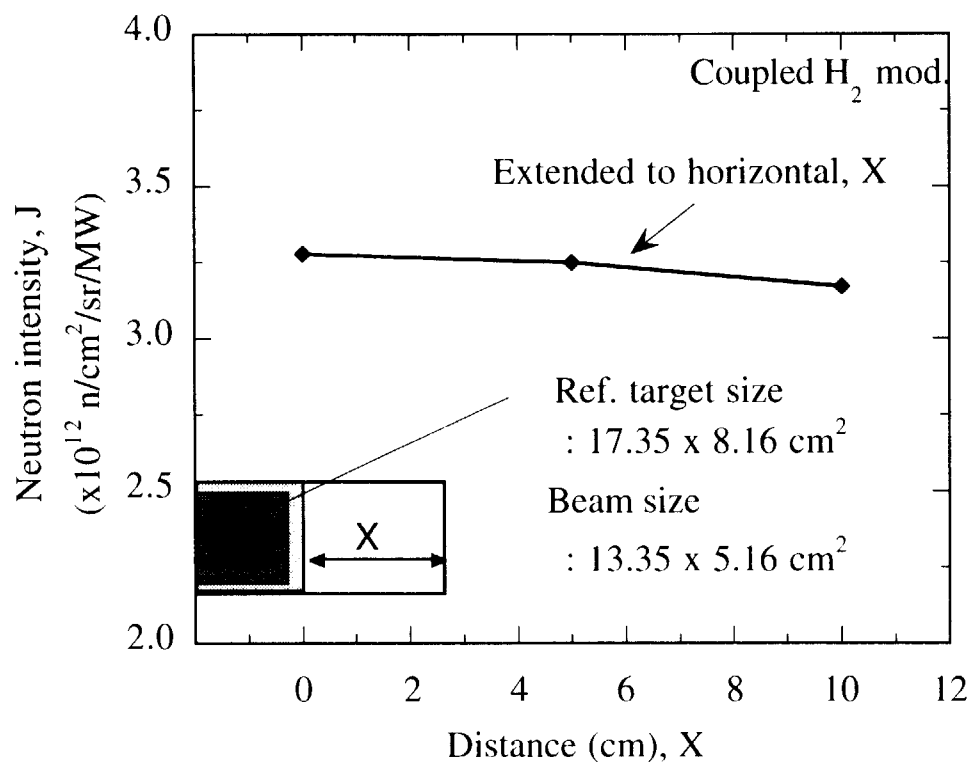


Fig. 11 Distance dependence of neutron intensity, J except reference target region

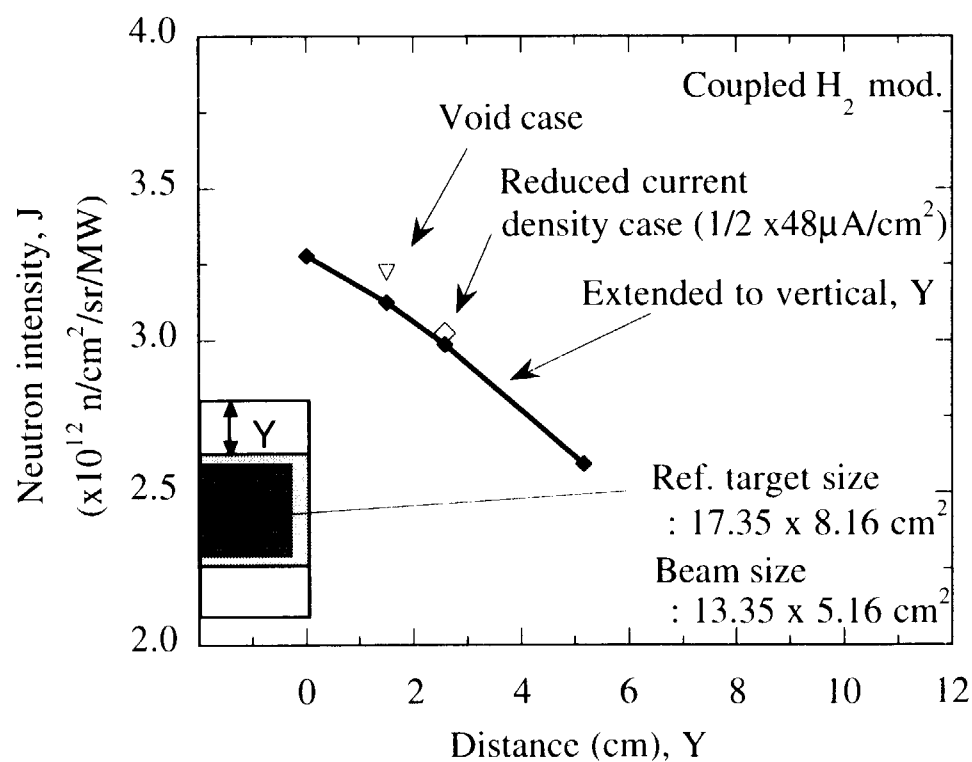


Fig. 12 Distance dependence of neutron intensity, J except reference target region

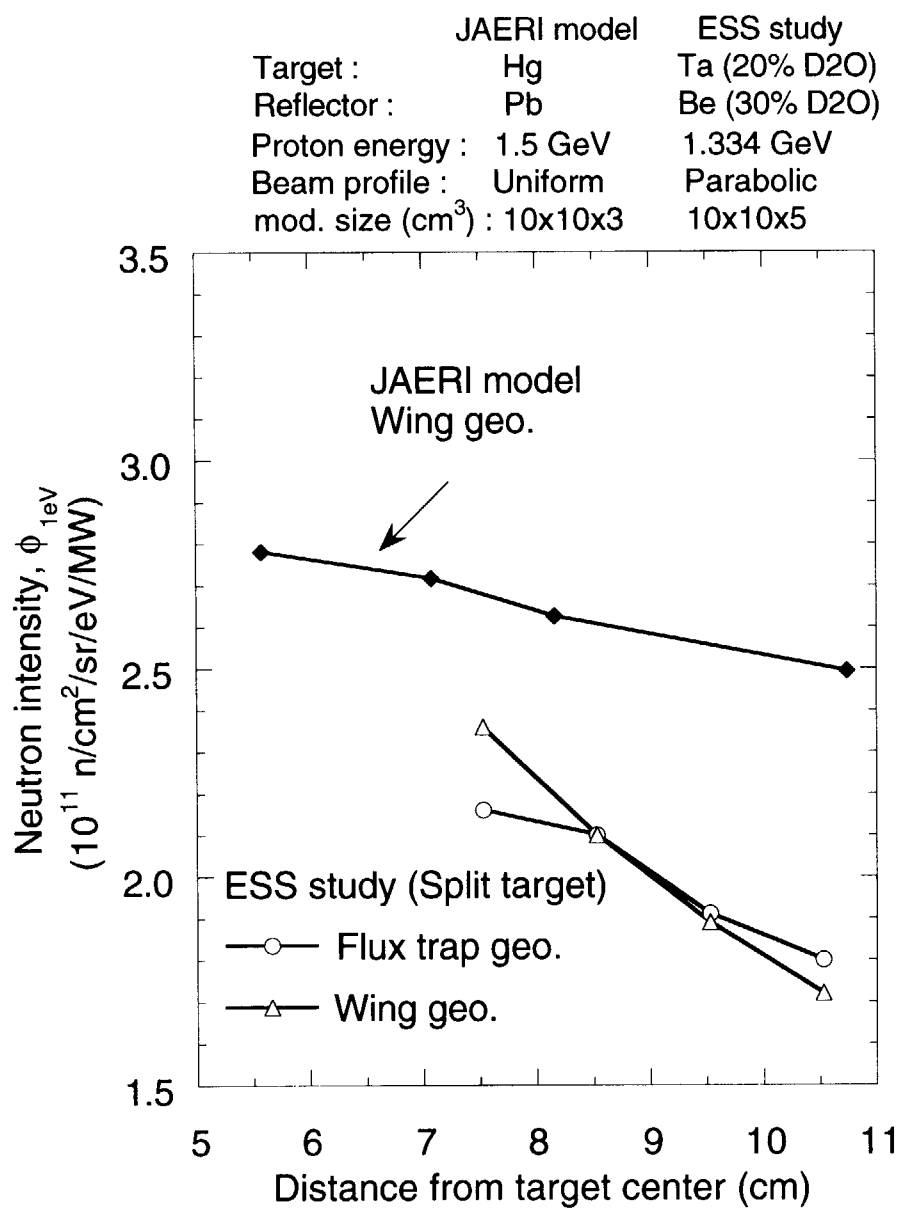


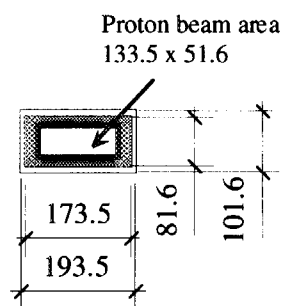
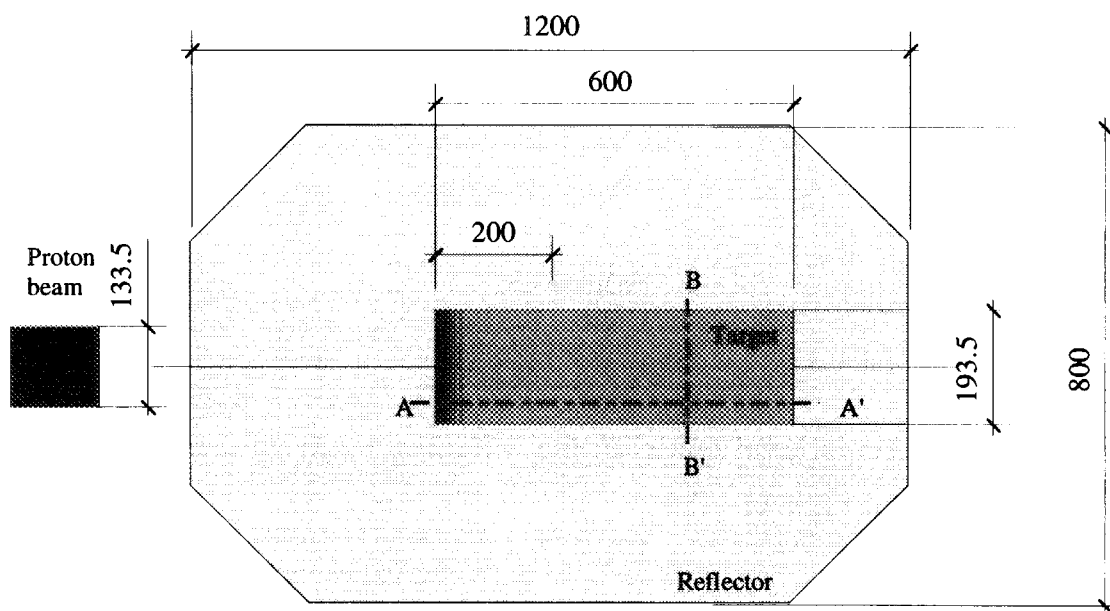
Fig. 13 Target shape effect on neutron intensity,  $\phi_{1\text{eV}}$ , from decoupled water moderator

This is a blank page.

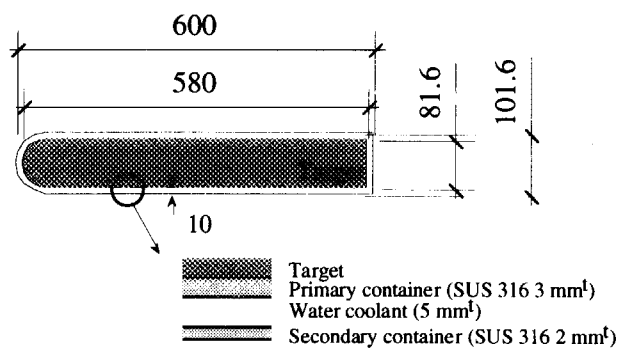


## Appendix

Details of the calculational model of the reference target-moderator-reflector system are shown in Figs A1 - A6.



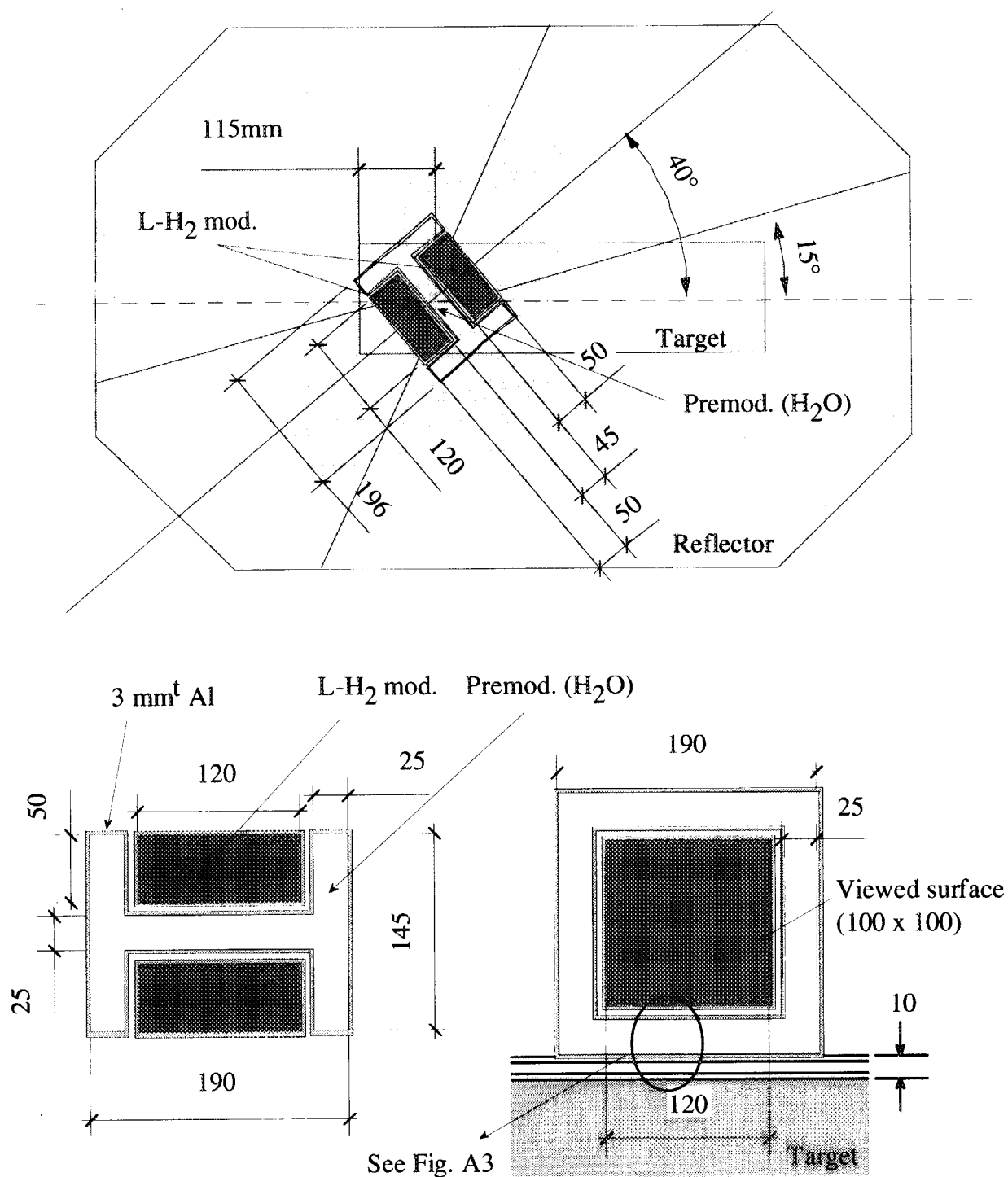
A - - - A' cross section of target



B - - - B' cross section of target

Unit : mm

Fig. A1 Layout and dimensions of target and reflector in calculational model



Unit : mm

Fig. A2 Detail layout and dimensions of L-H<sub>2</sub> moderators with premod. above target

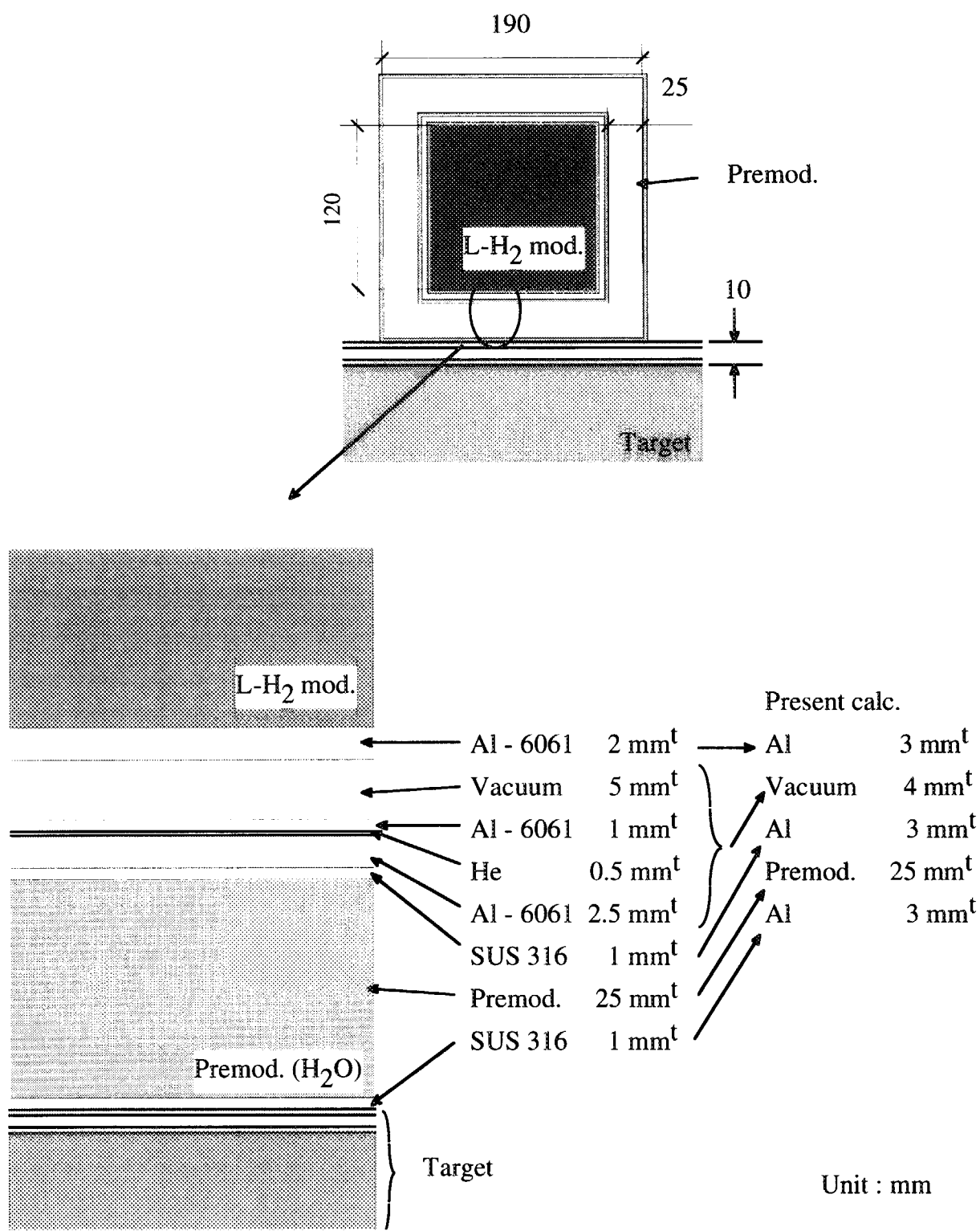
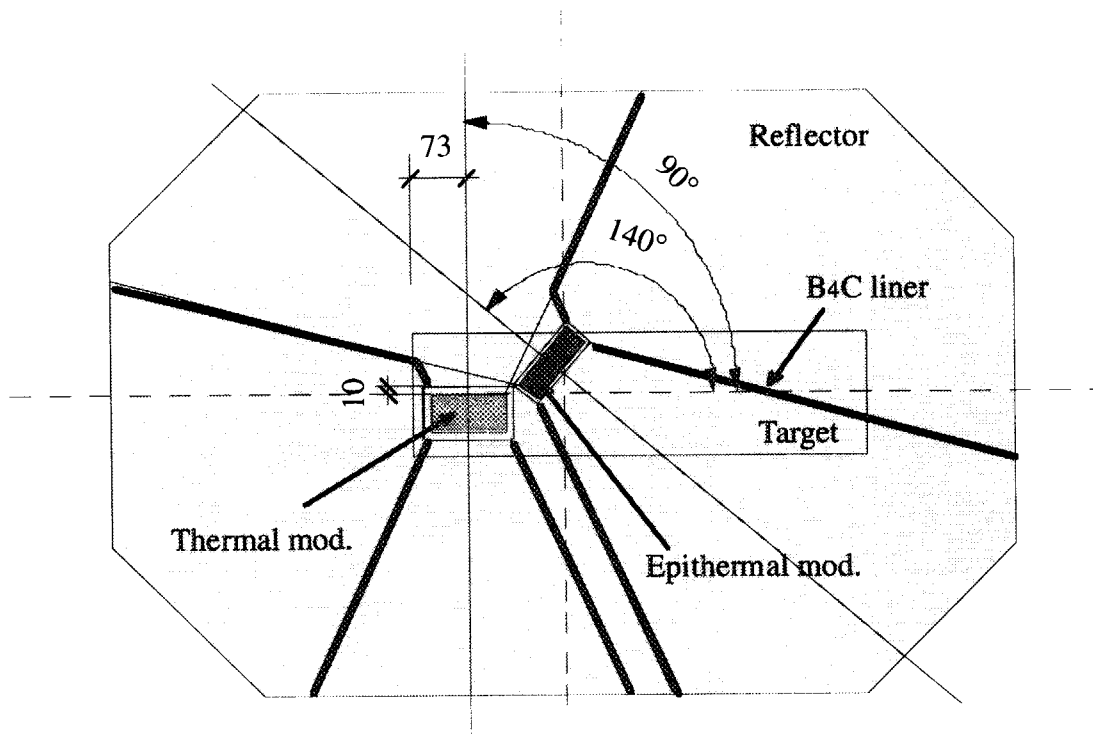


Fig. A3 Detail layout and dimensions of L-H<sub>2</sub> moderator with premod.



Unit : mm

Fig. A4 Detail layout and dimensions of thermal (cryogenic) and epithermal (H<sub>2</sub>O) moderators below target

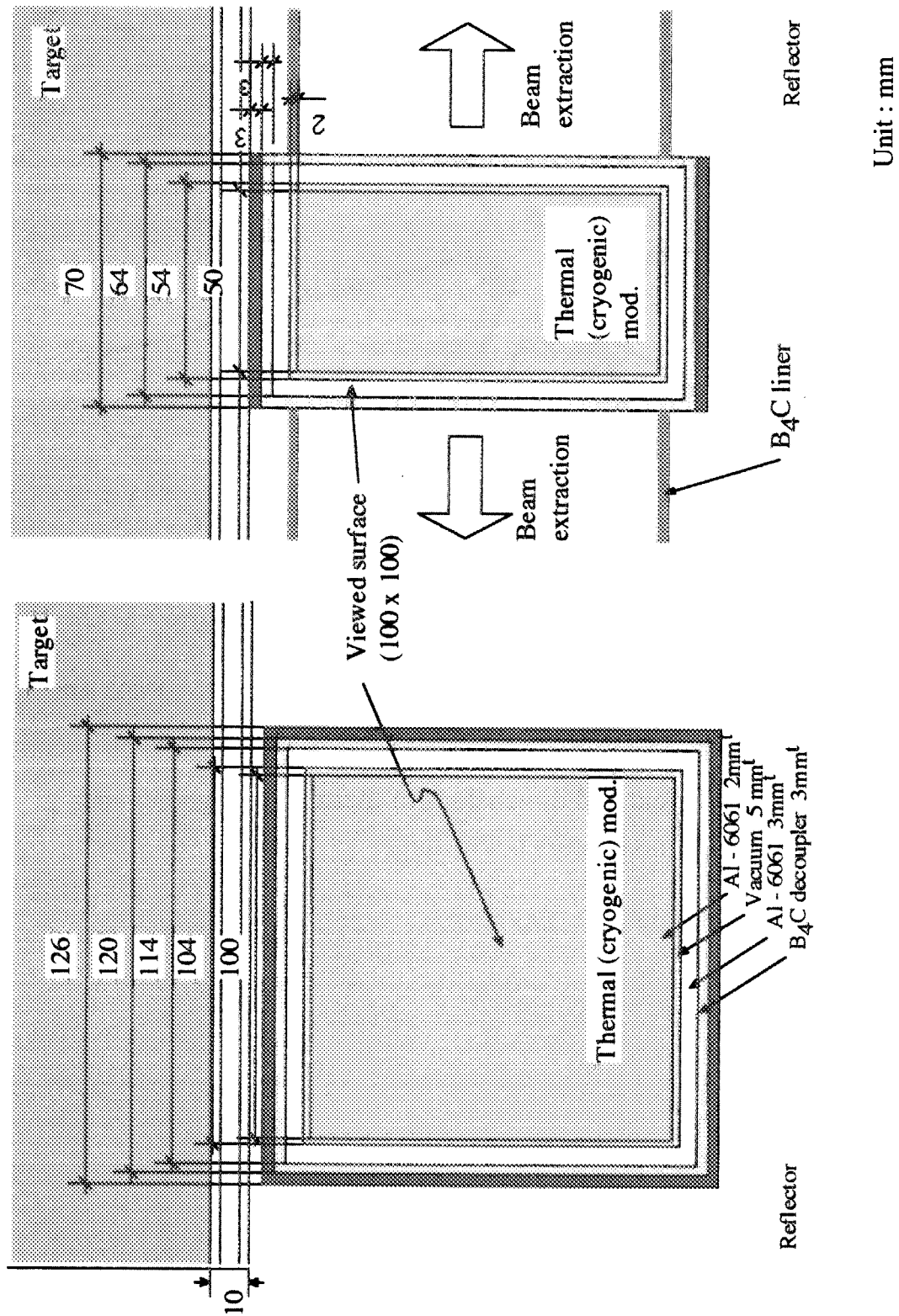


Fig. A5 Detail layout of thermal (cryogenic) moderator

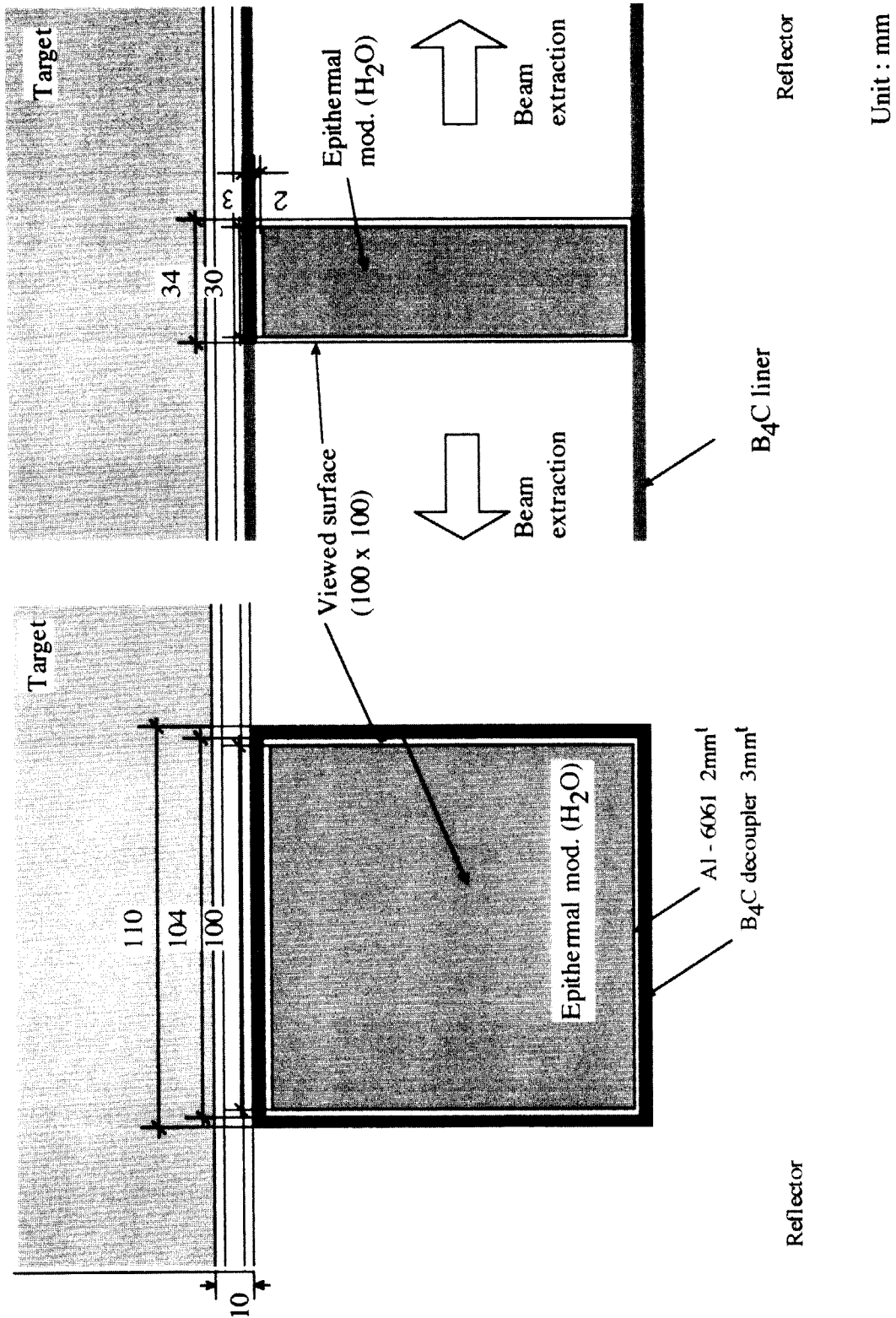


Fig. A6 Detail layout of epithermal moderator (H<sub>2</sub>O)

This is a blank page.



# 国際単位系 (SI) と換算表

表1 SI基本単位および補助単位

量	名称	記号
長さ	メートル	m
質量	キログラム	kg
時間	秒	s
電流	アンペア	A
熱力学温度	ケルビン	K
物質質量	モル	mol
光度	カンデラ	cd
平面角	ラジアン	rad
立体角	ステラジアン	sr

表3 固有の名称をもつ SI 組立単位

量	名称	記号	他の SI 単位 による表現
周波数	ヘルツ	Hz	$s^{-1}$
力	ニュートン	N	$m \cdot kg / s^2$
圧力, 応力	パスカル	Pa	$N / m^2$
エネルギー, 仕事, 熱量	ジュール	J	$N \cdot m$
工率, 放射束	ワット	W	$J / s$
電気量, 電荷	クーロン	C	$A \cdot s$
電位, 電圧, 起電力	ボルト	V	$W / A$
静電容量	ファラド	F	$C / V$
電気抵抗	オーム	$\Omega$	$V / A$
コンダクタンス	ジーメンズ	S	$A / V$
磁束	ウェーバ	Wb	$V \cdot s$
磁束密度	テスラ	T	$Wb / m^2$
インダクタンス	ヘンリー	H	$Wb / A$
セルシウス温度	セルシウス度	$^{\circ}C$	
光度	ルーメン	lm	$cd \cdot sr$
照射度	ルクス	lx	$lm / m^2$
放射能	ベクレル	Bq	$s^{-1}$
吸収線量	グレイ	Gy	$J / kg$
線量当量	シーベルト	Sv	$J / kg$

表2 SI と併用される単位

名称	記号
分, 時, 日	min, h, d
度, 分, 秒	$^{\circ}, ', ''$
リットル	l, L
トン	t
電子ボルト	eV
原子質量単位	u

$$1 \text{ eV} = 1.60218 \times 10^{-19} \text{ J}$$

$$1 \text{ u} = 1.66054 \times 10^{-27} \text{ kg}$$

表4 SI と共に暫定的に維持される単位

名称	記号
オングストローム	$\text{\AA}$
バ	b
バール	bar
ガリ	Gal
キュリー	Ci
レントゲン	R
ラド	rad
レム	rem

$$1 \text{ \AA} = 0.1 \text{ nm} = 10^{-10} \text{ m}$$

$$1 \text{ b} = 100 \text{ fm}^2 = 10^{-28} \text{ m}^2$$

$$1 \text{ bar} = 0.1 \text{ MPa} = 10^5 \text{ Pa}$$

$$1 \text{ Gal} = 1 \text{ cm/s}^2 = 10^{-2} \text{ m/s}^2$$

$$1 \text{ Ci} = 3.7 \times 10^{10} \text{ Bq}$$

$$1 \text{ R} = 2.58 \times 10^{-4} \text{ C/kg}$$

$$1 \text{ rad} = 1 \text{ cGy} = 10^{-2} \text{ Gy}$$

$$1 \text{ rem} = 1 \text{ cSv} = 10^{-2} \text{ Sv}$$

表5 SI接頭語

倍数	接頭語	記号
$10^{18}$	エクサ	E
$10^{15}$	ペタ	P
$10^{12}$	テラ	T
$10^9$	ギガ	G
$10^6$	メガ	M
$10^3$	キロ	k
$10^2$	ヘクト	h
$10^1$	デカ	da
$10^{-1}$	デシ	d
$10^{-2}$	センチ	c
$10^{-3}$	ミリ	m
$10^{-6}$	マイクロ	$\mu$
$10^{-9}$	ナノ	n
$10^{-12}$	ピコ	p
$10^{-15}$	フェムト	f
$10^{-18}$	アト	a

(注)

- 表1—5は「国際単位系」第5版, 国際度量衡局 1985年刊行による。ただし, 1 eV および 1 u の値は CODATA の 1986 年推奨値によった。
- 表4には海里, ノット, アール, ヘクタールも含まれているが日常の単位なのでここでは省略した。
- bar は, JIS では流体の圧力を表わす場合に限り表2のカテゴリーに分類されている。
- EC 閣僚理事会指令では bar, barn および「血圧の単位」mmHg を表2のカテゴリーに入れている。

換算表

力	N (=10 <sup>5</sup> dyn)	kgf	lbf
	1	0.101972	0.224809
	9.80665	1	2.20462
	4.44822	0.453592	1

$$\text{粘度 } 1 \text{ Pa} \cdot \text{s} (\text{N} \cdot \text{s} / \text{m}^2) = 10 \text{ P (ポアズ)} (\text{g} / (\text{cm} \cdot \text{s}))$$

$$\text{動粘度 } 1 \text{ m}^2 / \text{s} = 10^4 \text{ St (ストークス)} (\text{cm}^2 / \text{s})$$

圧	MPa (=10 bar)	kgf/cm <sup>2</sup>	atm	mmHg (Torr)	lbf/in <sup>2</sup> (psi)
	1	10.1972	9.86923	$7.50062 \times 10^3$	145.038
力	0.0980665	1	0.967841	735.559	14.2233
	0.101325	1.03323	1	760	14.6959
	$1.33322 \times 10^{-4}$	$1.35951 \times 10^{-3}$	$1.31579 \times 10^{-3}$	1	$1.93368 \times 10^{-2}$
	$6.89476 \times 10^{-3}$	$7.03070 \times 10^{-2}$	$6.80460 \times 10^{-2}$	51.7149	1

エネルギー・仕事・熱量	J (=10 <sup>7</sup> erg)	kgf·m	kW·h	cal (計量法)	Btu	ft·lbf	eV	1 cal = 4.18605 J (計量法)
	1	0.101972	$2.77778 \times 10^{-7}$	0.238889	$9.47813 \times 10^{-4}$	0.737562	$6.24150 \times 10^{18}$	= 4.184 J (熱化学)
	9.80665	1	$2.72407 \times 10^{-6}$	2.34270	$9.29487 \times 10^{-3}$	7.23301	$6.12082 \times 10^{19}$	= 4.1855 J (15 °C)
	$3.6 \times 10^6$	$3.67098 \times 10^5$	1	$8.59999 \times 10^5$	3412.13	$2.65522 \times 10^6$	$2.24694 \times 10^{25}$	= 4.1868 J (国際蒸気表)
	4.18605	0.426858	$1.16279 \times 10^{-6}$	1	$3.96759 \times 10^{-3}$	3.08747	$2.61272 \times 10^{19}$	仕事率 1 PS (仏馬力)
	1055.06	107.586	$2.93072 \times 10^{-4}$	252.042	1	778.172	$6.58515 \times 10^{21}$	= 75 kgf·m/s
	1.35582	0.138255	$3.76616 \times 10^{-7}$	0.323890	$1.28506 \times 10^{-3}$	1	$8.46233 \times 10^{18}$	= 735.499 W
	$1.60218 \times 10^{-19}$	$1.63377 \times 10^{-20}$	$4.45050 \times 10^{-26}$	$3.82743 \times 10^{-20}$	$1.51857 \times 10^{-22}$	$1.18171 \times 10^{-19}$	1	

放射能	Bq	Ci
	1	$2.70270 \times 10^{-11}$
	$3.7 \times 10^{10}$	1

吸収線量	Gy	rad
	1	100
	0.01	1

照射線量	C/kg	R
	1	3876
	$2.58 \times 10^{-4}$	1

線量当量	Sv	rem
	1	100
	0.01	1

(86年12月26日現在)

